

Experimental and theoretical investigation of planar polarization and radiation from plane-channeling relativistic electrons

S. A. Vorob'ev, E. G. Vyatkin, Yu. L. Pivovarov, A. P. Potylitsyn, and I. Khakberdiev

Nuclear Physics Research Institute of the Tomsk Polytechnic Institute

(Submitted 19 June 1987)

Zh. Eksp. Teor. Fiz. **94**, 38–50 (March 1988)

Results are presented of an experimental investigation of the spectral dependence of the linear polarization of radiation from 900-MeV electrons channeling in (110) planes of diamond and silicon crystals. The polarization characteristics of the radiation are calculated by modeling the particle trajectories in the crystal and by using a continuous model. The calculation results are compared with the experimental data and qualitative agreement is obtained. A high degree of linear polarization ($P \approx 0.6-0.8$) is noted at the spectral-dependence maximum whose position coincides with the maximum of the spectral density of the radiation.

I. INTRODUCTION

The study of relativistic particles in crystals is attracting much attention at present (see the reviews, Refs. 1–5). Sufficiently detailed studies, both theoretical and experimental, have been made of the spectral distribution of the radiation in axial and planar channeling of electrons and positrons of various energies. The more subtle polarization properties of this radiation have hardly been investigated, however. The first polarization measurements⁶ point to a high degree of linear polarization of the radiation for planar channeling of the electrons. Unfortunately, the degree of linear polarization $P = 0.65 \pm 0.15$ obtained in Ref. 6 is only an average over a rather wide spectral range (4–20 MeV). The aim of our present study is a more detailed experimental study of the spectral dependence of the linear polarization of the radiation for planar channeling of 900-MeV electrons in diamond and silicon crystals, and a theoretical interpretation of the results by modeling the spectra and all the Stokes parameters for the radiation. Computer modeling facilitates the study of the distinctive properties of spectra and of the Stokes parameters for typical electron trajectories in a crystal and the tracking of the formation of the observed spectral and polarization characteristics of the radiation after summing over all possible trajectories.

2. EXPERIMENT

The experiments were performed with the Tomsk "Sirius" synchrotron with the following beam characteristics: electron energy 900 MeV, monochromaticity $\lesssim 0.5\%$, intensity $\sim 2 \cdot 10^{10}$ e^- /cycle, dumping time $\tau = 18 \cdot 10^{-3}$ s, dumping frequency $f = 5$ Hz, and divergence at point of incidence on the target $\sim 10^{-4}$ rad. A diagram of the experimental setup is shown in Fig. 1.

The number of electrons was monitored by an inductive current sensor and a synchrotron-radiation detector prior to each dumping on the target. A goniometer made it possible to rotate the target about the vertical and horizontal axes in steps of 9° and 3° , respectively. The γ -ray beam was shaped by two collimators to an angular divergence $\theta_c = 0.2-0.6$ mrad, was rid of charged particles by a 0.8 T magnetic field, and fed through a vacuum duct into the experiment room, in which were installed a Compton polarimeter based on an NaI spectrometer (to record photons scattered at a given

polar angle) and a Gauss quantometer (to measure the total energy of the γ beam).

The polarimeter designed could measure simultaneously two polarization parameters describing the linear polarization of the photon beam in an energy interval from 1 to 30 MeV, viz., the degree P of photon polarization and the inclination angle φ_0 of the polarization plane, by measuring the azimuthal distributions of the scattered photons. To this end, the polarimeter was mounted on a special platform which permitted setting the polar angle of the detected scattered γ photons in an interval $\theta = 11-45^\circ$, and rotate the spectrometer around the γ -beam axis through $0-360^\circ$. The gamma spectrometer, based on an NaI(Tl) crystal 63 mm in diameter and 63 mm long, had a resolution 7.5% for the 1.33 MeV γ line from a Co^{60} source. To lower the stray background level, the γ detector was surrounded by a lead shield and connected for anticoincidence with a thin scintillation counter, to sift out events due to passage of charged particles through the detector radiator. The solid angle of the γ detector $\Delta\Omega = 1.3 \cdot 10^{-6}$ sr was determined by a cylindrical collimator 6 mm in diameter. The polarimeter scatterer was a polystyrene plate whose thickness was determined by experiment ($t = 2-10$ mm). The polarimeter was located in the photon beam in such a way that placing the γ detector at an azimuthal angle $\varphi = \pm 90^\circ$ corresponded to passage of the median plane of the synchrotron through the horizontal axis of the goniometer rotation.

The polarimeter sensitivity in a given photon energy interval is determined by the detection angle θ and by the differential cross section σ for Compton photon scattering.⁷

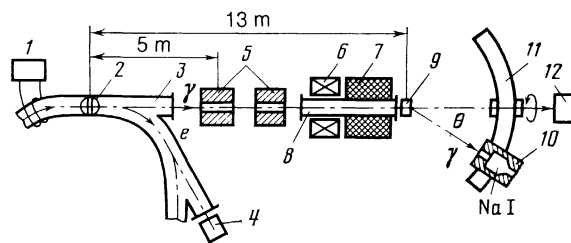


FIG. 1. Experimental setup: 1—inductive current sensor, 2—single-crystal target in goniometer, 3—accelerator exit tube, 4—synchrotron-radiation detector, 5—lead collimator, 6—clearing magnets, 7—lead-concrete shield, 8—vacuum channel, 9—scatterer, 10— γ spectrometer, 11—polarimeter rotating mechanism, 12—Gauss quantometer.

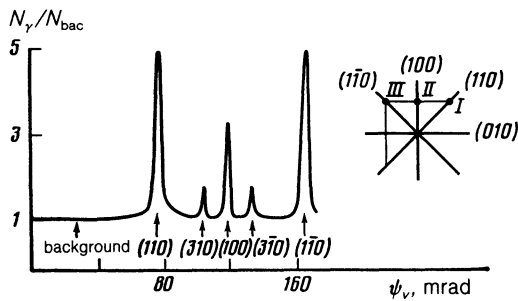


FIG. 2. Plot of orientation of the soft-photon yield from a diamond crystal ($t = 0.35$ mm) rotating around the vertical axis of the goniometer (φ_v) and "map" of crystallographic planes.

The polarization properties of the photons can be measured with least error when the maximum reduced analyzing ability σR^2 of the $\gamma + e \rightarrow \gamma' + e'$ process is reached. Here

$$R = (d\sigma_{\perp} - d\sigma_{\parallel}) / (d\sigma_{\perp} + d\sigma_{\parallel})$$

is the analyzing ability of the process, and $d\sigma_{\perp}$ and $d\sigma_{\parallel}$ are the differential cross sections for Compton scattering of photons polarized perpendicular and parallel to the reaction plane.⁷ The maximum of R for ~ 10 MeV photons is reached in this experiment at $\theta = 25^\circ$.

The crystal was oriented with the aid of the same spectrometer operating in the counting regime. Figure 2 shows typical orientation dependences of the spectrometer count on the angle of crystal rotation relative to the electron-beam direction, and a "map" of the crystallographic planes. The target-orientation accuracy was $\sim 7 \cdot 10^{-5}$ rad. It can be seen from Fig. 2 that even weak planes, such as (310) and (112), are distinctly identified, thus attesting to the reliability of this orientation procedure.

In addition to measuring the γ -ray polarization parameters, the procedure used permits simultaneous investigation of the spectral characteristics of the radiation. Figure 3 shows the intensity spectra of γ rays from a misoriented diamond crystal 0.35 mm thick. Curve 1 is the result of direct measurement of the spectrum with a NaI(Tl) spectrometer 200 mm in diameter and 200 mm long, while curve 2 was obtained by the developed procedure of reconstructing the spectrum of the scattered photons. The satisfactory agreement between curves 1 and 2 justifies the chosen procedure. The radiation spectrum of a misoriented crystal agrees in shape with the Schiff spectrum of radiation from an amorphous target.

The spectrometric information was accumulated in a

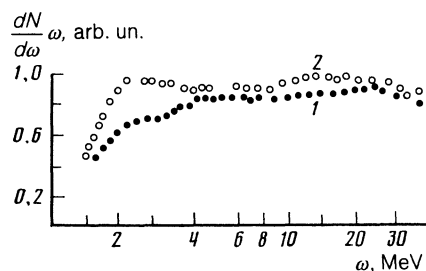


FIG. 3. Spectra of γ rays from a misoriented diamond crystal: curve 1—direct measurement results, 2—spectrum obtained after reduction.

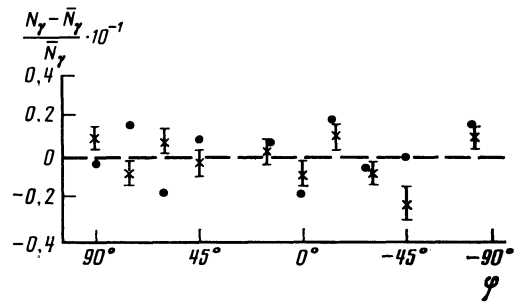


FIG. 4. Azimuthal distributions of photons scattered from an amorphous target (points) and from a misoriented crystal (crosses).

UNO-1024-90 multichannel analyzer, whose input was opened by a synchro-generator pulse during the time of electron dumping to the crystal ($\tau \approx 18$ ms). After subtracting the background (measured without a polystyrene scatterer), each spectrum was read and recorded on the disk of an IVK-3 computer assembly for further reduction.

To take into account the P and φ_0 measurement errors due to the instrumental asymmetry R' , control measurements were made with an amorphous target, as well as with misoriented crystals. It follows from Fig. 4 that the azimuthal dependences correspond to an isotropic distribution and that $R' = 0$ within the limits of error.

In the experiment with a diamond single crystal $t = 0.35$ mm thick, the information was accumulated in the primary-photon energy intervals $\hbar\omega = 1-3$, $3-7$, and $7-20$ MeV for the case of electron motion along the planes (100) and (110). Figure 5 shows the azimuthal dependence of the yield of scattered photons of energy $\hbar\omega' = 2-3$ MeV (corresponding to the primary-photon energy interval $\hbar\omega = 3-7$ MeV) for electron channeling in the (110) plane. The figure shows also a fit equation of the type

$$N(\varphi) = A_0 + A_1 \cos 2\varphi + A_2 \sin 2\varphi. \quad (1)$$

The obtained coefficients A_i ($i = 0, 1, 2$) were used to determine the degree of polarization P , given the energy interval and the slope angle φ_0 between the plane of maximum linear polarization and the horizontal reference plane:

$$P = \frac{(A_1^2 + A_2^2)^{1/2}}{\bar{R}A_0}, \quad \varphi_0 = \frac{1}{2} \operatorname{arctg} \left(\frac{A_2}{A_1} \right). \quad (2)$$

Here \bar{R} is the analyzing ability of the process, averaged for

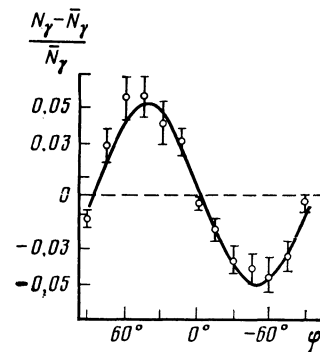


FIG. 5. Azimuthal dependences of the yield of scattered photons with initial energy $3 < \omega < 7$ MeV, produced in (110)-plane channeling of electrons in a crystal of thickness $t = 0.35$ mm (points), and the result of fitting to a trigonometric polynomial (solid curve).

TABLE I. Experimental values of the degree of linear polarization of radiation and results of computer modeling for 900-MeV electrons for (100)-plane channeling in diamond.

$\Delta\hbar\omega$, MeV	$\langle \xi_s(\Delta\omega) \rangle$	
	Experiment	Modeling
1-3	0.61 ± 0.10	0.245
3-7	0.66 ± 0.13	0.647
7-20	0.61 ± 0.17	0.570
4-20	0.65 ± 0.17	0.593

the specified photon-energy interval, and calculated in accordance with Ref. 7 for a scattering angle $\theta = 25^\circ$. The results of the measurements of P for diamond in certain energy intervals are listed in Table I. The values of the degree of polarization for a silicon crystal of thickness $t = 0.4$ mm are given in Table II. The directions of the planes (110), (100), and (1 $\bar{1}$ 0), determined from the obtained values of the angles $\varphi_0 = -42.3 \pm 1.7^\circ$; $\varphi_0 = 90 \pm 2.5^\circ$ and $\varphi_0 = 46 \pm 1.5^\circ$, agree within the limits of error with the directions of the plane on the "map" of Fig. 3. Experiment attests to observation of a spectral dependence of the degree of linear polarization of the electron emission, for planar channeling in diamond and silicon under conditions of strong collimation of the radiation. A physical interpretation of this interesting result is given below (see Secs. 3 and 4).

To verify the influence of the crystal thickness on the spectral and polarization properties of the radiation, measurements similar to those described above were made for a diamond crystal of thickness $t = 10$ mm (0.078 radiation lengths). The polystyrene scatterer of the polarimeter was a cylinder of 10 mm diam and 10 mm long, corresponding to an effective collimation 0.4 rad of the γ beam. The measured azimuthal dependence of the photons in the energy interval $\hbar\omega = 1-15$ MeV are given in Fig. 6. The values of P and φ_0 were 0.80 ± 0.15 and $76 \pm 3^\circ$, as against $P = 0.25 \pm 0.1$ for photons of energy $\hbar\omega = 15-30$ MeV. The radiation preserves thus a high degree of linear polarization even in sufficiently thick crystals (under strong collimation conditions) in the case of planar channeling. This may indicate that in crystals whose thickness exceeds the dechanneling length by more than two decades the character of the spectral dependence of the radiation polarization is determined by the electron channel proper (up to thicknesses comparable with the dechanneling length), and beyond this by capture in the bulk.^{8,9}

The experimental data indicate thus that γ beams of high intensity and considerable degree of linear polarization can be relatively easily obtained in the case of planar channeling of electrons in perfect single crystals.

TABLE II. Experimental values of the degree of linear polarization of radiation of 900-MeV electrons for (110)-plane channeling in silicon.

$\Delta\hbar\omega$, MeV	$\langle \xi_s(\Delta\omega) \rangle$
0.64-2.0	0.504 ± 0.05
2-3	0.629 ± 0.08
3-7	0.451 ± 0.04
7-15	0.434 ± 0.06
15-37	0.125 ± 0.03

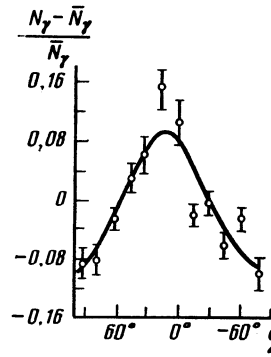


FIG. 6. Azimuthal dependence of the yield of scattered photons with initial energy $1 < \omega < 15$ MeV, produced in (110)-plane channeling of electrons in a diamond single crystal of thickness $t = 10$ mm, and the results of the fitting.

3. INTERPRETATION OF DATA BY MODELING THE SPECTRAL AND POLARIZATION PROPERTIES OF THE RADIATION

An appropriate computer experiment was undertaken for a physical interpretation of the experimental data. In Sec. 3.1 below we describe briefly the principles of the model, and in Sec. 3.2 we give the results for typical trajectories of planar channeling electrons.

3.1. Binary model for the calculation of the radiation properties

The properties of the radiation of relativistic particles in a crystal are obtained with the aid of the standard binary model.¹⁰⁻¹² The trajectories $\mathbf{r}(t)$ and the particle velocity $\beta = \mathbf{v}(t)c^{-1}$ in the crystal are obtained with the aid of the binary model (using the Moliere atomic potential in the calculation of the scattering angle). These values are substituted in the known classical electrodynamics equations for the radiation intensity.¹³ After integrating by parts we can obtain from these equations the following expressions:

$$\frac{d^2\epsilon}{d\omega d\Omega} = \frac{e^2}{2\pi^2c} |[(\mathbf{l}_1 + \mathbf{l}_2)\mathbf{n}]|^2, \quad (3)$$

$$\mathbf{l}_1 = -i\omega \int_{t_1}^{t_2} dt \beta(t) \exp\left[i\omega\left(t - \frac{\mathbf{nr}(t)}{c}\right)\right], \quad (4)$$

$$\mathbf{l}_2 = \frac{\beta(t_2) \exp[i\omega(t_2 - \mathbf{nr}(t_2)/c)]}{[1 - \mathbf{n}\beta(t_2)]} - \frac{\beta(t_1) \exp[i\omega(t_1 - \mathbf{nr}(t_1)/c)]}{[1 - \mathbf{n}\beta(t_1)]}. \quad (5)$$

Here ω and \mathbf{n} are the frequency and the emission direction of the photon, t_1 and t_2 are the instants of the first and last collisions of the particle with the crystal atoms. In Eq. (3), \mathbf{l}_1 describes the radiation inside the crystal, \mathbf{l}_2 takes boundary effects into account, and a term appears also as a result of the interference of these two types of radiation.

The polarization properties of the radiation are completely described by the polarization matrix¹³ $d\epsilon_{ik} = I_0 \rho_{ik}$, where I_0 is the total radiation intensity. The matrix ρ_{ik} can be expressed in terms of the Stokes parameters ξ_i ($i = 1, 2, 3$):

$$\rho_{ik} = \frac{1}{2} \begin{pmatrix} 1 + \xi_3 & \xi_1 - i\xi_2 \\ \xi_1 + i\xi_2 & 1 - \xi_3 \end{pmatrix}. \quad (6)$$

The Stokes parameters are quadratic combinations of the field-strength components E_λ ($\lambda = 1, 2$) with a definite linear polarization λ

$$\xi_1 = \frac{E_1 E_2^* + E_1^* E_2}{I_0}, \quad i\xi_2 = \frac{E_1^* E_2 - E_1 E_2^*}{I_0}, \quad (7)$$

$$\xi_3 = \frac{|E_1|^2 - |E_2|^2}{I_0}, \quad I_0 = |E_1|^2 + |E_2|^2.$$

The maximum degree of the linear polarization¹³ is $P = (\xi_1^2 + \xi_2^2)^{1/2}$, and the degree of the circular polarization is characterized by the Stokes parameter ξ . The angle φ , which determines the direction of the maximum linear polarization in a plane perpendicular to the photon emission angle, is defined by $\tan(2\varphi) = \xi_1/\xi_3$. The field components E_λ are determined with the aid of the polarization vectors e_λ and, accurate to within constants that are immaterial for the determination of ξ_i , are given by

$$E_\lambda = e_\lambda (I_1 + I_2). \quad (8)$$

In (8), I_1 and I_2 are determined by computer modeling using Eqs. (4) and (5).

We shall use the set of polarization vectors e_λ adopted in the theory of synchrotron (undulator) radiation, since an analogy can be drawn between the radiation from a particle in a spiral (planar) undulator and the radiation in axial (planar) channeling. If s is a unit vector in the direction chosen in the problem, then

$$e_1 = \frac{[ns]}{[1 - (n \cdot s)^2]^{1/2}}, \quad e_2 = \frac{n(ns) - s}{[1 - (n \cdot s)^2]^{1/2}}, \quad (9)$$

$$n = [e_1, e_2], \quad ne_1 = ne_2 = e_1 e_2 = 0.$$

Choosing $s \parallel x$ (Fig. 7), we obtain for emission "forward" (at an angle $\theta = 0$, for which the computer experiment was performed) $n = \{0, 0, 1\}$, $e_1 = \{0, 1, 0\}$, $e_2 = \{-1, 0, 0\}$. It follows from (3)–(5) and (8) that the components E_1 and E_2 for "forward" radiation are determined by the transverse velocity components $\beta_y(t)$ and $\beta_x(t)$ of the particle in the crystal.

An important feature of the problem is the formation of the observable radiation properties via summation over all possible trajectories; this is attained by adding the intensities (3) from individual trajectories. Recognizing that there is no interference of radiation along different trajectories, it is

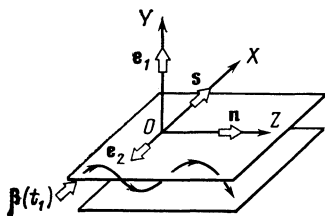


FIG. 7. The coordinate frame used in the computer experiment with the position of the initial velocity $\beta(t)$ and the unit vector s . The photon-emission direction and the polarization vectors $e_{1,2}$ are given for $\theta = 0$.

easy to show that the averaging of the Stokes parameters ξ_i when summing over different trajectories should follow the scheme

$$\langle \xi_i(\omega, n) \rangle = \sum_{k=1}^N \xi_i^k(\omega, n) W_k(\omega, n), \quad (10)$$

where

$$W_k = (|E_1^k|^2 + |E_2^k|^2) / \sum_{j=1}^N (|E_1^j|^2 + |E_2^j|^2)$$

is the relative contribution made to the total observed intensity (at the frequency ω and in the direction n) from the k th trajectory; $\xi_i^k(\omega, n)$ is the Stokes parameter for the k th trajectory.

3.2. Spectral and polarization properties of radiation for characteristic trajectories

The computer experiment was carried out for planar channeling of 900-MeV electrons along (110) and (100) planes of diamond and silicon. The particle distribution in emission angle was assumed Gaussian with a mean value $\bar{\theta}_0 = 0$ and a variance $(\bar{\theta}^2)^{1/2} \approx 10^{-5}$ rad, which amounted to $\sim 0.1 \psi_L$ for the indicated planes (ψ_L is the Lindhard critical angle). It can be concluded from the simulation data that in crystals of thickness not larger than the dechanneling length one can determine the below- and above-barrier motion (using the terminology of the continuous model) and the mixed type of motion with transition from one type to the other. In thicker crystals, as shown in Ref. 14, strong mixing prevents the separation of the purely below- and above-barrier states.

Figure 8 shows one of the characteristic below-barrier electron trajectories for (110)-plane channeling in diamond, and the corresponding spectrum ($\theta = 0$) and Stokes parameters of the radiation from this trajectory. It follows from an analysis of the projections of the trajectory on the YZ and XZ planes (Figs. 8a, b) that the real trajectory, unlike in the continuous models, is not a plane curve. Moreover, the amplitude and the frequency ω^* of the electron oscillations in the channel are substantially changed (Figs. 8a, b) on passing through the crystal, owing to the short-range collisions with the atoms and to multiple scattering. These properties of the real trajectory influence the spectrum and the polarization characteristics of the radiation.

Actually, the theory^{15,16} predicts for radiation at an angle $\theta = 0$ the existence of only odd harmonics (if the boundary effect is disregarded). The width of these harmonics is $\Gamma_N \sim 2\gamma^2 \hbar \omega^* n/N$, where N is the total number of oscillations in the channel, and $n = 1, 3, 7, \dots$. The continuous model for a trajectory with the same initial values of $r(t)$ and $\beta(t_1)$ as shown in Fig. 8 leads to $\Gamma_N \approx 0.5\text{--}0.6$ MeV. The real spectrum (Fig. 8c) is more complicated in view of the changes of ω^* . In fact, the widths of the first three observable harmonics in Fig. 8c, near 5, 15, and 25 MeV, is much larger than Γ_N . Moreover, since the final value of ω^* is double the initial, new harmonics are produced in the region of each initial ω^* , with frequencies up to twice as high (Fig. 8c).

Motion of particles in planar channeling is usually described in theoretical papers with the aid of the potential

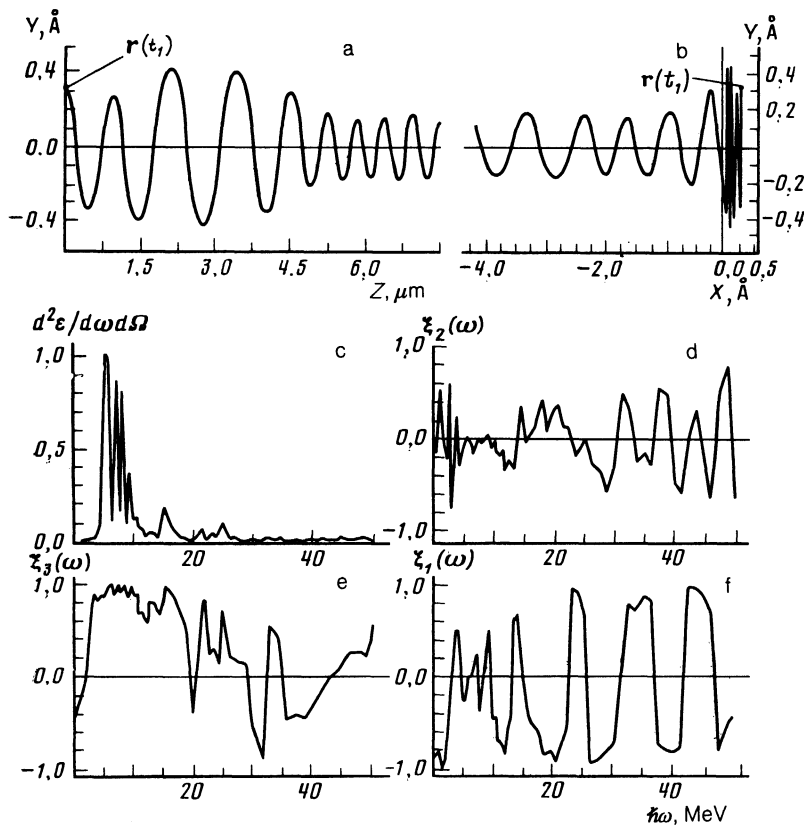


FIG. 8. Projections of a trajectory, typical of (110)-plane channeling of 900-MeV electrons in diamond, on the planes YZ (a) and XZ (b) ($r(t_i)$ is the entry point), the radiation spectrum (c), and the three Stokes parameters (d-f). The intensity spectrum is normalized to the maximum, the crystal thickness is $t = 10 \mu\text{m}$, and the temperature is $T = 0$. The angle with the $\langle 110 \rangle$ axis is 40 mrad.

$V(y)$ of the crystallographic planes.¹⁻⁴ In these papers (see also Refs. 15 and 16), $\beta_x(t) = \text{const}$ and therefore radiation in the specified direction $\theta = 0$ is fully linearly polarized, i.e., $\xi_3^k(\omega, \theta = 0) = 1$ for each trajectory, and consequently also $\langle \xi_3^k(\omega, \theta = 0) \rangle = 1$. For a real trajectory, both β_y and β_x depend on the time, and this leads to a more complicated dependence of the Stokes parameters on the photon frequency, Figs. 8d-f. The Stokes parameters $\xi_1(\omega)$ and $\xi_2(\omega)$ oscillate rapidly with change of ω . The maximum of the Stokes parameter $\xi_3(\omega)$, Fig. 8d, correlates well with the principal maximum of the radiation spectrum, Fig. 8c, thus attesting to a high degree of linear polarization of the radiation in the region typical of the channeling maximum. The oscillations of $\xi_1(\omega)$ and $\xi_2(\omega)$ turn out to be substantial when averaged over the various trajectories, see Sec. 4 below.

As to the above-barrier trajectories, simulation shows that the projection of a trajectory of this type on a plane is similar to that obtained from the continuous model,^{15,16} whereas the motion in the XZ plane turns out to be rather complicated. As a result, the radiation spectrum is complicated, but the radiation is highly polarized as before. Spectra of radiation from mixed-type trajectories are characterized by the presence of frequencies observable in the spectra of both below- and above-barrier particles.

4. COMPARISON OF THE EXPERIMENTAL AND OF THE MODELING RESULTS

The observed radiation spectra and Stokes parameters are the results of summation and averaging over the trajectories (see Sec. 3.1). The radiation spectra obtained by modeling in accordance with the procedure described above agree in form with experiment.¹⁷ This comparison was carried out in our earlier work.^{19,20} The form of the radiation

spectrum¹⁷ can also be well described by using the continuous approximation for planar channeling with allowance for multiple scattering.¹⁸ We shall therefore dwell in greater detail on a comparison of the experimental results with the theory, for the degree of linear polarization of radiation of 900-MeV electrons in (110)-plane channeling in diamond and silicon.

Figure 9 shows plots of $\langle \xi_3^k(\omega, \theta = 0) \rangle = 1$ for radiation of (110)-plane channeling 900-MeV electrons in diamond. Curves 1 and 2 were obtained using the equations of Refs. 16 and a potential of the "inverted parabola" type. Curve 1 was calculated with an initial electron beam divergence $\Delta_0 = 10^{-4}$ rad, and curve 2 with an angular divergence corresponding to multiple scattering in a target 350 μm thick

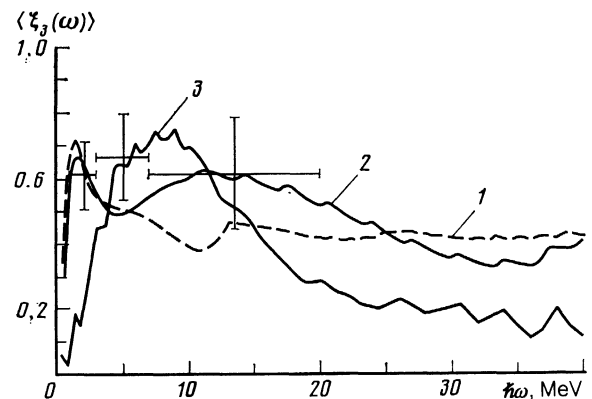


FIG. 9. Curve 3—Stokes parameter $\langle \xi_3(\omega) \rangle$ for the emission spectrum at (110)-plane channeling of 900-MeV electrons in diamond, obtained by modeling ($t = 10 \mu\text{m}$); Curves 1 and 2—calculation using the continuous model.¹⁶ Crosses—data or our experiment.

$\langle \xi_3^k(\omega, \theta = 0) \rangle = 1 \text{ rad}$). Curve 3 was obtained by simulating with 900 trajectories tracked to a depth $10 \mu\text{m}$, and the crosses are the results of our experiment.

In the computer experiment the angles between the entering particles and the $\langle 110 \rangle$ and $\langle 100 \rangle$ axes in the channeling plane were $\varphi = 40 \text{ mrad}$, and the crystal temperature was $T = 203 \text{ K}$. The entrance angles θ_0 were the same as in Sec. 3.2. The position of the maximum in the radiation spectrum (given in Ref. 17) correlates well with the position of the maximum of the Stokes parameter $\langle \xi_3(\omega) \rangle$ in Fig. 9, curve 3. In this spectral range the radiation is linearly polarized to a high degree. The Stokes parameters $\langle \xi_1(\omega) \rangle$ and $\langle \xi_2(\omega) \rangle$, averaged over all the trajectories are close to zero and are not cited here. This is a consequence of the rapid oscillations of $\xi_1^k(\omega)$ and $\xi_2^k(\omega)$ for the individual trajectories, see Fig. 8. Thus, the total radiation of 900-MeV electrons in $\langle 110 \rangle$ channeling in diamond does not have circular polarization, $\langle \xi_2(\omega) \rangle \approx 0$, and the direction of the maximal linear polarization practically coincides with the normal to the $\langle 110 \rangle$ plane, so that $\langle \xi_1(\omega) \rangle \approx 0$.

From a comparison of the curves of Fig. 9 with the experimental data it follows that both the theory¹⁸ and the modeling lead to the conclusion that the degree of linear polarization of electron radiation in planar channeling has a characteristic spectral dependence. No full agreement between the modeling data, the analytic calculations, and experiment was reached, see Fig. 9. The reason is the following. The parameter $\langle \xi_3(\omega) \rangle$ was calculated (curves 1 and 2) using equations¹⁶ obtained for the description, in the dipole approximation, of the polarization properties of electron radiation in thin crystals. Therefore a comparison of the calculated and experimental results can be only illustrative in character, since a complete theoretical description of the polarization properties of radiation in channeling should allow for collimation and for multiple scattering in a "thick" crystal, as was done in the comparison of the theoretical and experimental results on the radiation spectra in Ref. 18. Suitable corrections should be introduced into the modeling procedure to be able to deal with larger thicknesses and to take collimation of the radiation into account. One should expect to obtain along these lines a complete description of the polarization properties of radiation in the case of planar channeling.

All the foregoing holds also for the silicon data shown

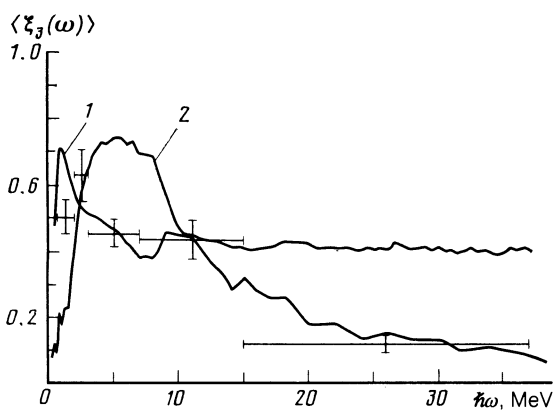


FIG. 10. Curve 2—Stokes parameter $\langle \xi_3(\omega) \rangle$ for radiation of $\langle 110 \rangle$ -plane-channeling 900-MeV electrons in silicon. Curve 1—calculation using the continuous model.¹⁶ Crosses—our experimental data.

in Fig. 10. Here curve 1 shows the result of calculation by using the equations of Ref. 16, curve 2 the modeling results, and the crosses the experimental data (see Sec. 2) for the degree of linear polarization of 900-MeV electrons channeled along $\langle 110 \rangle$ in silicon. In the simulation, $t = 16 \mu\text{m}$ and $T = 293 \text{ K}$, and in the experiment $t = 400 \mu\text{m}$. It follows from Fig. 10 that simulation describes the experimental data better, although there is no full agreement.

In the experiment (Sec. 2), the measured quantity was $\langle \xi_3(\Delta\omega) \rangle$ averaged over definite spectral bands $\Delta\omega$ (see Tables I and II). To obtain these values from the modeled values of Figs. 9 and 10 it is necessary to integrate the polarization matrix $d\omega$ over the angle subtended by the detector and over the spectral interval $\Delta\omega$, find the Stokes parameters for each trajectory, and then average over all the trajectories. The result of the calculations is

$$\langle \xi_i(\Delta\omega, \Delta\Omega) \rangle = \int_{\Delta\omega} \int_{\Delta\Omega} d\omega d\Omega \langle \xi_i(\omega, \Omega) \rangle \alpha(\omega, \Omega), \quad (11)$$

$$\alpha(\omega, \Omega) = \left\{ \int_{\Delta\omega} \int_{\Delta\Omega} d\omega d\Omega \sum_{k=1}^N [|E_1^k|^2 + |E_2^k(\omega, \Omega)|^2] \right\}^{-1} \times \sum_{k=1}^N \{ |E_1^k(\omega, \Omega)|^2 + |E_2^k(\omega, \Omega)|^2 \},$$

where $d(\omega, \Omega)$ is the relative contribution in Ω of the radiation intensity at the frequency ω to the total radiation intensity in the spectral band $\Delta\omega$ and in the solid angle $\Delta\Omega$. In Eqs. (11), $\langle \xi_i(\omega, \Omega) \rangle$ is determined from Eq. (10) and represents the Stokes parameter for radiation at the frequency ω in the solid angle Ω , averaged over all the trajectories. The values calculated with the aid of (11)

$$\langle \xi_3(\Delta\omega) \rangle = P(\Delta\omega)$$

are given for the case of $\langle 110 \rangle$ channeling in diamond in Table I together with the experimental data, with which they agree satisfactorily notwithstanding the large differences in the crystal thicknesses used in the modeling and in the real experiment.

A complete description of the experimentally obtained polarization properties of radiation in planar channeling of relativistic electrons calls thus for additional advances in the theory as well as for further improvement of the modeling procedure. It would be of interest at the same time to carry out a cycle of analogous experiments on thinner crystals.

5. CONCLUSION

The experimental and theoretical investigation of the spectral and polarization characteristics of radiation by 900-MeV electrons in planar channeling in diamond and silicon allow us to draw the following conclusions.

1. The degree of linear polarization of radiation in planar channeling has a characteristic dependence on the photon frequency, with a pronounced maximum whose position coincides with that of the maximum of the radiation spectrum.

2. For planar channeling, the radiation near the characteristic maximum is linearly polarized with a high degree of polarization, $P \approx 0.6-0.8$.

An interesting result of the modeling is observation of a substantial change of the electron-oscillation frequency in the planar channel, which leads to a broadening of the radiation spectrum. On the other hand, a change of the oscillation frequency hinders greatly various methods of stimulating his radiation by external electromagnetic fields. It is interesting to note that the position of the maximum in the radiation spectra coincides with the region of giant dipole resonance for photonuclear reactions. This makes possible a detailed study of nuclear structure with the aid of photonuclear reactions initiated by linearly polarized photons.

The following further research projects are promising. First, investigation of the orientational dependence of the polarization with a transformation of the radiation by channeling, at large θ_0 and φ_0 , into coherent bremsstrahlung. Second, investigation in the quantum region, i.e., at electron energy $E_0 < 100$ MeV. These two cases, and also a more detailed study of the polarization characteristics of the radiation in channeling as functions of the planar-target thickness and temperature (of particular interest is channeling near (111) binary planes) are attractive objects of further theoretical and experimental study. These investigations are important for the development of intense sources of monochromatic photons with high degree of linear polarization and easily controllable energy for experimental nuclear physics.

The authors thank N. F. Shul'ga, V. I. Truten', S. P. Fomin, and B. I. Shramenko for helpful comments, and also V. M. Katkov for an interesting discussion.

- ¹R. Wedell, Phys. Stat. Sol. (b) **99**, 11 (1980).
- ²A. I. Akhiezer and N. F. Shul'ga, Usp. Fiz. Nauk **137**, 561 (1982) [Sov. Phys. Usp. **25**, 541 (1982)].
- ³V. A. Bazylev and N. K. Zhevago, *ibid.* p. 605 [565].
- ⁴V. V. Beloshitsky and F. F. Komarov, Phys. Rept. **21**, 304 (1983).
- ⁵J. C. Cimbball and N. Cue, Phys. Rept. **21**, 304 (1983).
- ⁶Yu. N. Adishchev, I. E. Vnukov, S. A. Vorob'ev, *et al.*, Pis'ma Zh. Eksp. Teor. Fiz. **33**, 478 (1981) [JETP Lett. **33**, 462 (1981)].
- ⁷A. I. Akhiezer and V. B. Berestetskii, Quantum Electrodynamics, [in Russian], Nauka 1969. Transl. of earlier ed., Interscience, 1965.
- ⁸A. M. Taratin and S. A. Vorob'ev, Pisma Zh. Tekh. Fiz. **10**, 102 (1984) [Sov. Tech. Phys. Lett. **10**, 42 (1984)].
- ⁹V. A. Muravlev, Dokl. Akad. Nauk SSSR **284**, 1107 (1985) [Sov. Phys. Dokl. **30**, 861 (1985)].
- ¹⁰V. V. Kudrin, Yu. A. Timoshnikov, and S. A. Vorobiev, Phys. Stat. Sol. (b), **58**, 409 (1973).
- ¹¹E. G. Vyatkin and Yu. L. Pivovarov, Izv. Vyssh. Ucheb. Zaved. Fizika **8**, 78 (1983).
- ¹²E. G. Vyatkin and Yu. L. Pivovarov, *ibid.*, **8**, 83 (1983); **11**, 63 (1986).
- ¹³V. N. Baïer, V. M. Katkov, and V. S. Fadin, Radiation from Relativistic Electrons [in Russian]. Atomizdat, 1973.
- ¹⁴V. A. Bazylev, V. I. Glebov, and V. V. Golovizin, Zh. Eksp. Teor. Fiz. **91**, 25 (1986) [Sov. Phys. JETP **64**, 14 (1986)]. Dokl. Akad. Nauk SSSR **288**, 105 (1986) [Sov. Phys. Doklady **31**, 410 (1986)].
- ¹⁵M. A. Kumakhov, Phys. Lett. **A57**, 17 (1976).
- ¹⁶V. N. Baïer, V. M. Katkov, and V. M. Strakhovenko, Preprints No. 79-7 and 80-03, Inst. Nucl. Phys. Siberian Div., USSR Acad. Sci., (1979 and 1980).
- ¹⁷Yu. N. Adishchev, I. E. Vnukov, S. A. Vorob'ev, *et al.*, Dokl. Akad. Nauk SSR **268**, 841 (1983) [Sov. Phys. Doklady **28**, 144 (1983)].
- ¹⁸V. N. Baïer, V. M. Katkov, and V. M. Strakhovenko, *ibid.* **268**, 1365 (1983) [**28**, 167 (1983)].
- ¹⁹E. G. Vyatkin, Yu. L. Pivovarov, and S. A. Vorobiev, Nucl. Instr. Meth. **B17**, 30 (1986).
- ²⁰E. G. Vyatkin, Yu. L. Pivovarov, and S. A. Vorobiev, Nucl. Phys. **284B**, 509 (1987).

Translated by J. G. Adashko